Spring magnet behavior in $DyFe_2/YFe_2$ Laves phases superlattices

K. Dumesnil, M. Dutheil, C. Dufour, and Ph. Mangin
Laboratoire de Physique des Matériaux (UMR 7556), Université H. Poincaré-Nancy I, Boîte Postale 239, 54506 Vandoeuvre les Nancy Cedex, France
(Received 21 March 2000)

Original composite systems with two isomorphous Laves phases ($DyFe_2$ and YFe_2) have been elaborated by molecular-beam epitaxy. These superlattices combine the hard magnetic properties of $DyFe_2$ with the soft ones of YFe_2. Moreover, they exhibit high single-crystal quality and constitute model systems to investigate the influence of the relative energy terms on the magnetization reversal. The magnetization measurements show that it is thus possible to tailor the magnetic configuration and the magnetization reversal process. Particularly interesting behaviors have been observed in the superlattice [$DyFe_2$(50 Å)/YFe_2(130 Å)], which presents spring ferrimagnet characteristics, together with an exchange bias of the hysteresis loop. The bias can be either positive or negative, depending on the cooling-field value and, therefore, shows memory of the magnetic history of the superlattice. The spring-magnet loop appears to be reversible over the (−7.5 T/+7.5 T) field range at low temperature.

An interesting way to extend the already large amount of magnetic materials, and to tailor their magnetic behavior, is to turn to composite materials, thus taking advantage of the specific magnetic properties of each component. So, now emerging are the so-called exchange spring magnets,[1] which are composed of a fine mixture of a hard and a soft magnetic material. In such systems, the magnetization of the hard magnetic material is tightly stuck along easy directions, whereas the magnetization of the soft magnetic material can be turned by a small external magnetic field. However, because of the exchange coupling at the interfaces between both phases, the magnetization of the soft material is recalled along the magnetization direction of the hard material. Therefore, there is a significant field range where the magnetic behavior is perfectly reversible; the magnetic domain walls that develop at the interfaces act as recall springs. So the magnetic configuration in such systems is the result of the balance between the anisotropy energy (mainly in the hard material), the energy of the interfacial domain walls, and, when an external magnetic field is applied, the Zeeman energy in both components.

Because of the potential application of such composite systems in the field of high-performance permanent magnets, an increasing amount of studies is devoted to these spring magnets. Most of the systems have been fabricated by rapid quenching and subsequent annealing or mechanical alloying to form a nanocomposite with randomly oriented hard grains.[2] After the theoretical calculation performed by Skomski and Coey[3] on the exchange hardening of nanostructured systems composed of an *aligned* hard phase and a soft phase, multilayer structures composed of alternating hard and soft magnetic regions have been elaborated.[4] Some trilayer amorphous systems, which associate hard and soft intermetallic compounds of transition metals and rare earths,[5,6] have been also studied. Recently, Fullerton *et al.*[7] pointed out the interest of the epitaxied systems such as superlattices, where the crystallographic coherence allows for the investigation of the role of crystal orientation and structure, and permits much more easily aligned hard magnetic layers. Moreover, if the components are isomorphous, high-quality interfaces can be expected, and the superlattices then constitute model systems to study the effects related to the interfaces and to the relative thicknesses of each component.

In this paper, we present results concerning the magnetic properties of a composite system that is a superlattice constituted of two isomorphous intermetallic compounds with the $C15$ Laves phases structure ($DyFe_2$ and YFe_2). Because of the anisotropic electron $4f$ cloud of dysprosium, $DyFe_2$ is a hard magnetic material, which is also strongly magnetostrictive.[8] It is ferrimagnetic, with an average magnetic moment at low temperature of $2.2\mu_B$/atom [$(\mu_{Dy} - 2\mu_{Fe})/3$] along the dysprosium moments, the iron magnetic moments being antiparallel to the dysprosium ones. Yttrium is a nonmagnetic element, and YFe_2 is a soft compound with an average magnetic moment of $0.9\mu_B$/atom, along the iron moments [$(\mu_Y - 2\mu_{Fe})/3$]. The coupling between $DyFe_2$ and YFe_2 occurs at the interface through the positive exchange between iron magnetic moments of both components, and through the negative coupling between iron (of YFe_2) and dysprosium moments. These exchange couplings lead to a net antiparallel coupling between $DyFe_2$'s and YFe_2's magnetization, and the system is thus a kind of giant ferrimagnet.

In zero magnetic field, the expected magnetic configuration is that sketched in Fig. 1(a) and, depending on the relative thicknesses of each compound, the net magnetization is along the dysprosium or the iron moments. Under an external magnetic field, the net magnetization could orient along the field direction, preserving the relative magnetic configurations of the layers. Alternatively, the Fig. 1(a) magnetic configuration can be broken with the orientation of the net magnetization of each layer along the field and, therefore, with the creation of interfacial domain walls [Fig. 1(b)]. In Fig. 1(b) the total magnetization of the sample is larger than in the previous configuration [Fig. 1(a)]. From the relative exchange and anisotropy constants in $DyFe_2$ and YFe_2, the wall energy is expected to be 20 times larger in $DyFe_2$ than in YFe_2, and the magnetic walls are thus expected to form in the soft YFe_2 layers.

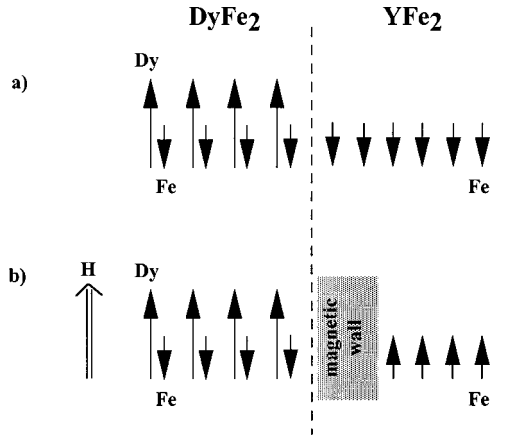

FIG. 1. Sketched magnetic configurations for a $DyFe_2/YFe_2$ interface (a) under zero magnetic field and (b) under high magnetic field.

We present here various magnetization reversal processes that have been tailored in these composite epitaxied systems by changing the relative thicknesses of both components: the superlattice can behave as a single hard magnetic compound that switches as a unit, as a mixture of two rather independent compounds, or, more surprisingly, as a spring ferrimagnet over the $(-7.5\ \mathrm{T}/+7.5\ \mathrm{T})$ field range. In this third case, the initial magnetic configuration under 7.5 T can be chosen via the cooling procedure, and the low-temperature hysteresis loop thus shows memory of the magnetic history of the superlattice.

The samples were prepared on $(11\bar{2}0)$ sapphire substrates by molecular-beam epitaxy, in a high vacuum chamber whose base pressure is typically 4×10^{-11} Torr. A buffer composed of a (110) 500 Å niobium layer covered by a very thin iron film (15 Å) was first deposited onto the substrate.[9] The role of this thin iron deposition is to initiate the following RFe_2 epitaxy (R=Y or Dy).

The YFe_2 and $DyFe_2$ layers were then obtained by alternative codeposition of Fe and Y, and Fe and Dy. The samples were finally coated with a 200 Å thick yttrium layer to prevent them from oxidation. Yttrium and niobium were evaporated from electron guns, dysprosium and iron from Knudsen cells. The evaporation rates were controlled and calibrated from quartz balances and optical captors.

The growth mode and the crystal quality of the surface have been checked with an *in situ* reflection high energy electron diffraction (RHEED) setup. The Laves phase compounds present the following epitaxial relationships with niobium:[9]

$$[001]_{DyFe_2}\|[001]_{YFe_2}\|[001]_{Nb}$$

$$\text{and } [1\bar{1}0]_{DyFe_2}\|[1\bar{1}0]_{YFe_2}\|[1\bar{1}0]_{Nb}.$$

After the deposition of the superlattice, the RHEED patterns (Fig. 2) exhibit continuous, thin, and contrasted streaks, which reveal a high crystal quality and a rather smooth surface. The compound stoichiometry has been checked by microanalysis, and is within $\pm2\%$ of the expected value.

The large-angle x-ray diffraction patterns (Fig. 3) exhibit satellites, indicated by arrows, due to the chemical modulation of the sample (i.e., a bilayer thickness). This confirms the periodicity of the stacking. Moreover, the full width at half maximum of the rocking curve measured across the (220) main Bragg peak (see inset in Fig. 3) leads to a mosaic spread of approximately 1.3°, which indicates a high degree of crystalline orientation.

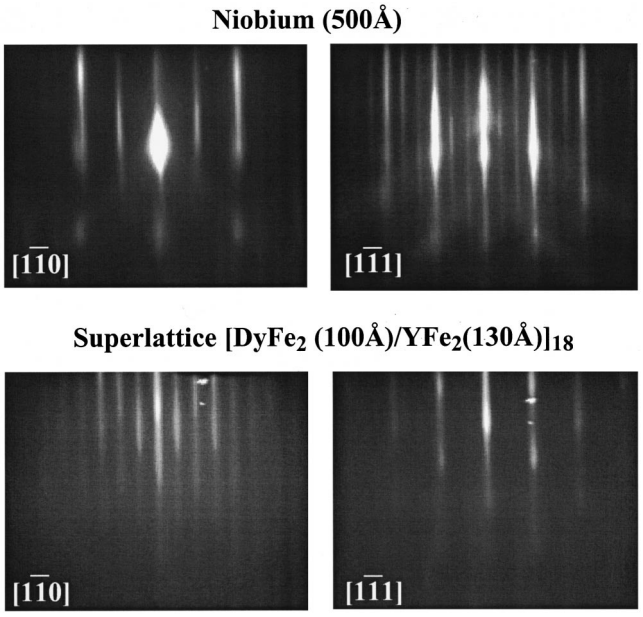

FIG. 2. RHEED patterns measured along the $[1\bar{1}0]$ and $[11\bar{1}]$ azimuthal directions after the deposition of the 500 Å thick niobium buffer, and after the deposition of the $[DyFe_2(100\,\text{Å})/YFe_2(130\,\text{Å})]_{18}$ superlattice.

The magnetic properties have been investigated by superconducting quantum interference device measurements for three typical superlattices with different relative thicknesses:

superlattice A, $[DyFe_2(50\,\text{Å})/YFe_2(130\,\text{Å})]_{21}$,

superlattice B, $[DyFe_2(100\,\text{Å})/YFe_2(130\,\text{Å})]_{18}$,

superlattice C, $[DyFe_2(100\,\text{Å})/YFe_2(50\,\text{Å})]_{26}$,

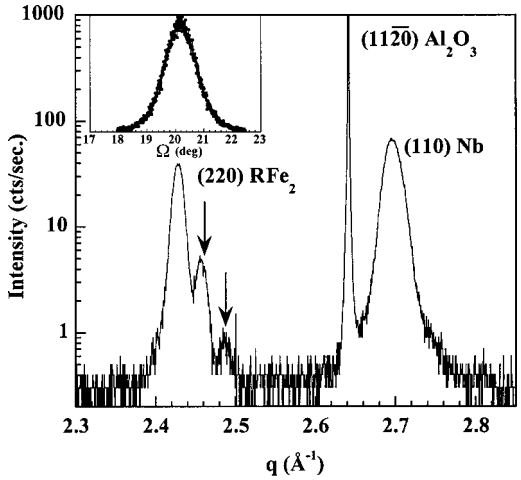

FIG. 3. Large-angle x-ray diffraction pattern for the $[DyFe_2(100\,\text{Å})/YFe_2(130\,\text{Å})]_{18}$ superlattice. Arrows indicate the satellites due to the chemical modulation. The rocking curve across the (220) main Bragg peak is given in the inset.

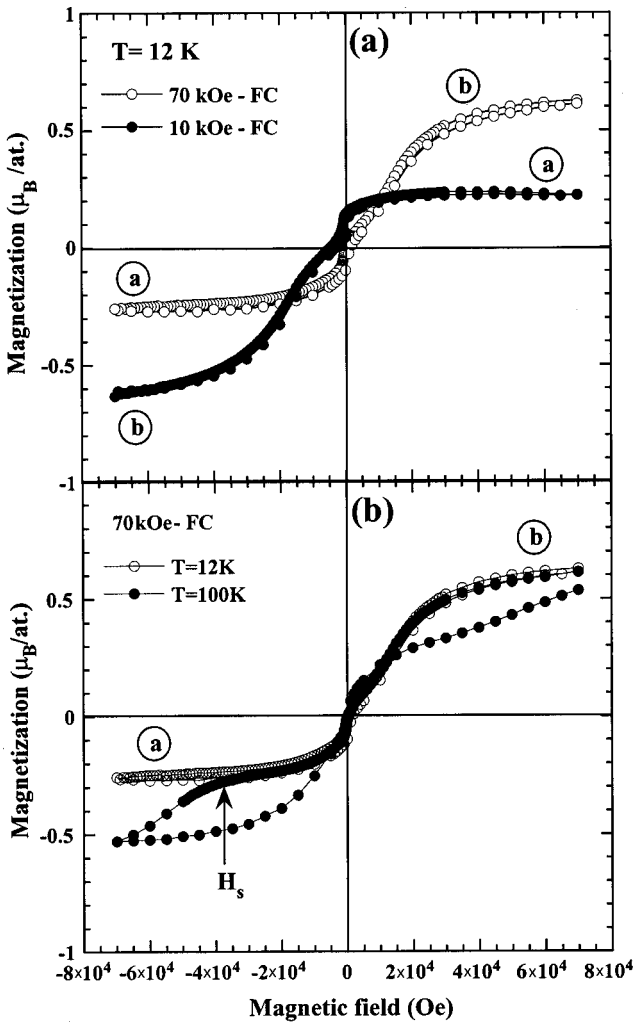

FIG. 4. Hysteresis loops measured for the superlattice $[DyFe_2(50\,Å)/YFe_2(130\,Å)]_{21}$: (a) At 12 K after two different cooling processes; after cooling the sample from room temperature under 10 kOe [10 kOe-FC (black dots)] and under 70 kOe [70 kOe-FC (white dots)]. (b) At 12 K (white dots) and at 100 K (black dots) after cooling under 70 kOe from room temperature. [The letters *a* and *b* presented in circles refer to the magnetic configurations sketched in Figs. 1(a) and 1(b), respectively. H_s is the magnetic field at which the $DyFe_2$ magnetization starts to switch.]

The measurements have been performed with the magnetic field applied along different in-plane crystallographic directions: [001], $[1\bar{1}0]$, and $[11\bar{1}]$. For the three samples, the $[1\bar{1}0]$ direction appears to be the easy magnetization direction in $DyFe_2$, especially at high temperatures. This is different from the bulk $DyFe_2$ magnetic behavior, which presents $\langle 001\rangle$ easy axis at any temperature.[8] However, this is in agreement with a study that we performed on $DyFe_2$ thin epitaxied films.[10] Only the results collected with the magnetic field applied along the $[1\bar{1}0]$ in-plane direction are therefore presented in the following.

Two magnetic loops collected at 12 K from superlattice *A* $[DyFe_2(50\,Å)/YFe_2(130\,Å)]$ are shown in Fig. 4(a). The magnetization unit has been chosen in Bohr magneton per atom. The curves have been collected after cooling the sample from room temperature under two different magnetic fields: under +10 kOe (+10 kOe-FC represented by black dots) and under +70 kOe (+70 kOe-FC represented by white dots). It is remarkable that each of the curves is very asymmetric, reversible, and that the two curves are symmetric to each other about the origin point.

The reversibility of the magnetization reversal at low temperature is interpreted by the blocking of the magnetization of the 50 Å $DyFe_2$ layers. The difference between the loops reveals that the 70 kOe and the 10 kOe field cooling bring the system into two different magnetic configurations. The 70 kOe field cooling brings the system in the configuration sketched in Fig. 1(b), where the net magnetizations of both compounds are aligned with the field direction. The energy cost to form the interface magnetic walls is compensated by the gain in Zeeman energy obtained by the alignment of the net magnetizations in the core of each layer.

When the superlattice is cooled under 10 kOe, the gain in Zeeman energy obtained for the configuration in Fig. 1(b) would be too small, and in any case, insufficient to drive the development of interface magnetic walls. So the sample behaves as a homogeneous system whose net magnetization aligns along the field direction; this brings the system into a configuration that is symmetric with the one in Fig. 1(a): because of the small $DyFe_2$ thickness, the iron magnetic moments are dominant and are thus all aligned with the external magnetic field, the dysprosium ones being antiparallel.

Consequently, two different magnetic states can be achieved by cooling in a 10 kOe or 70 kOe applied field: the $DyFe_2$ magnetization is quenched either along the cooling field direction (70 kOe-FC), or in the opposite direction (10 kOe-FC). Once the cooling procedure is finished, the $DyFe_2$ magnetization is determined and fixed; the application of a 7.5 T magnetic field at low temperature drives only the YFe_2 moments along the field direction, and thus two different magnetic configurations can be stabilized, depending on the cooling field magnitude. They differ by the $DyFe_2$ magnetization direction, lead to different magnetization values, and show a memory of the magnetic history of the superlattice. This memory effect is stabilized by the strong anisotropy in the $DyFe_2$ thin layers at low temperature.

To further demonstrate the memory effect, we have also cooled the sample under −70 kOe and under −10 kOe. The −70 kOe field cooling leads to the same loop as the +10 kOe field cooling, whereas the −10 kOe field cooling leads to the same loop as the +70 kOe field cooling. This is in perfect agreement with the above interpretation: the −70 kOe field cooling quenches *the net* $DyFe_2$ *magnetization* along negative fields, and the initial magnetic configuration (under +7.5 T) thus corresponds to Fig. 1(a); the −10 kOe field cooling quenches the *iron moments* along negative fields (i.e., the net $DyFe_2$ magnetization along positive fields), and the initial magnetic configuration (under +7.5 T) thus corresponds to Fig. 1(b).

The nonhysteretic evolution of the magnetization versus magnetic field is due to the reversal process that only involves extension or compression of magnetic walls in the soft YFe_2 layers, whereas the $DyFe_2$ magnetization direction does not change in the entire field range. The loops are characteristic of a spring ferrimagnet, with a very large magnetic field range within which the magnetization is reversible: the

soft phase will spring back into alignment with the hard phase once the applied field is removed.

For the system cooled under 70 kOe, the frozen magnetic configuration is unstable because the exchange interface interaction is frustrated and the walls thus extend as soon as the magnetic field decreases. They extend until the system reaches the configuration shown in Fig. 1(a) for negative fields. For the 10 kOe cooling, the frozen magnetic configuration is stable with respect to exchange: iron moments are aligned in both compounds, along the field direction. This prevents the domain wall extension for positive fields and leads to a higher remanence state; the walls begin to form only for negative fields and compress when increasing the field, so that more and more iron moments (in YFe_2) are aligned with the field.

It is interesting to notice that, due to the memory effect, the asymmetry of the hysteresis loop (i.e., the reversal field) changes sign with the magnitude of the cooling field: this is similar to exchange biasing effects observed in FeF_2/Fe bilayers.[11] In this system, the interface exchange interaction between FeF_2, [antiferromagnetic (AFM)] and Fe, [ferromagnetic (FM)], is antiferromagnetic, and the exchange bias results from a competition between this interface interaction and the external field/AFM surface magnetic coupling interaction. If the cooling field is large enough to align the AFM surface magnetization, the AFM/FM exchange interaction is frustrated and the system is in a state of high interface magnetic energy; this leads to a positive exchange bias field. The exchange bias field is negative if the cooling field is not large enough to overcome the interface antiferromagnetic interaction.

Our case is very close to this, since there is a net antiparallel coupling between $DyFe_2$'s and YFe_2's magnetization, and the system can be field-cooled into either a low- or a high-interface magnetic energy configuration, depending on the magnitude of the cooling field. The main difference lies in the fact that $DyFe_2$ is a ferrimagnetic compound whose resulting magnetization is different from zero and thus strongly coupled to the external applied field; a magnetically uncompensated surface is not necessary. An accurate investigation of the achieved magnetic state versus the cooling field value should also bring valuable information on the exchange coupling at the interfaces.

When the superlattice is cooled from room temperature to 100 K under 70 kOe [Fig. 4(b)], the results are very similar to those collected at low temperature, except that the reversible range is reduced: the magnetization of the 50 Å $DyFe_2$ layers can be reversed under a field smaller than the maximum 75 kOe available. Part of the loop presents now a hysteretic behavior, when the field is decreased once the $DyFe_2$ magnetization started to reverse. The irreversibilities are therefore clearly related to the $DyFe_2$ magnetization reversal. Let's note, however, that the $DyFe_2$ reversal is not complete since the loop is still asymmetric.

For thicker $DyFe_2$ layers [superlattice *B* $DyFe_2$ (100 Å)/YFe_2 (130 Å)], the hysteresis loops measured at 12 K and at room temperature after zero field cooling are presented in Fig. 5. In contrast to the previous results, two different steps obviously occur when the field decreases, even at low temperature. At 75 kOe, the configuration is the one sketched in Fig. 1(b), with the net magnetization of both

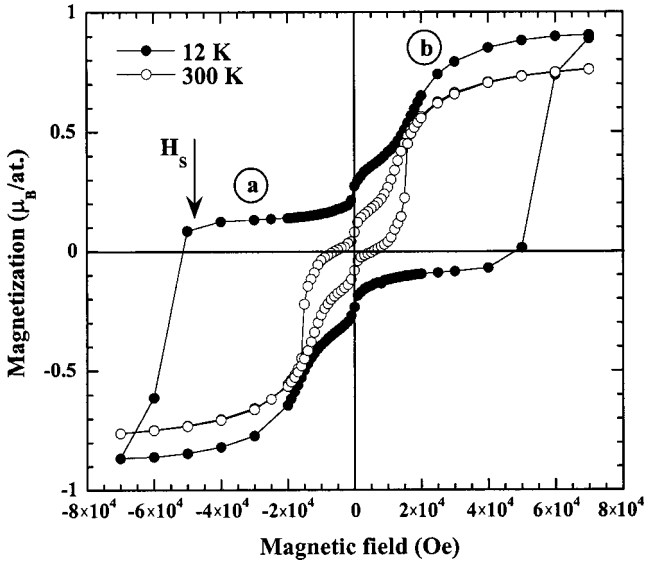

FIG. 5. Hysteresis loops measured at 12 K (black dots) and at room temperature (white dots) for the superlattice $[DyFe_2(100\,Å)/YFe_2(130\,Å)]_{18}$. The letters *a* and *b* presented in circles refer to the magnetic configurations sketched in Figs. 1(a) and 1(b), respectively. H_s is the magnetic field at which the $DyFe_2$ magnetization starts to switch.

compounds along the field direction and domain walls at the interfaces, on the YFe_2 side. In decreasing the magnetic field from +75 kOe to zero, the domain walls extend, so at zero field the configuration is that of Fig. 1(a). This configuration is stuck by the magnetically hard $DyFe_2$ layer from $H=0$ to the field H_s for which the $DyFe_2$ magnetization switches. H_s decreases when the temperature increases, as expected from the decreasing crystal-field anisotropy. Let us also underline that, when the temperature increases, the amplitude for the slow decrease of magnetization under positive magnetic field (between 75 and 5 kOe) does not change, whereas the amplitude of the abrupt variation at H_s significantly decreases. This has to be related to the thermal evolution of the dysprosium and iron magnetic moments. The iron Curie temperature being larger than the dysprosium one, the variation of magnetization due to the magnetic walls in YFe_2 does not vary, whereas the drop due to the $DyFe_2$ magnetization reversal decreases.

The two-step reversal observed in sample *B* is due to the fact that the switching field requested in these 100 Å $DyFe_2$ layers is 55 kOe at 12 K, whereas it is larger than 75 kOe for 50 Å $DyFe_2$ layers (sample *A*), consistent with the study we performed on the magnetic anisotropy in unique $DyFe_2$ films.[12] This feature makes it impossible to freeze a stable magnetic state (with respect to exchange interactions) at low temperature and under high magnetic field, as it was the case for the previous superlattice. Although with thicker layers and much smaller characteristic fields, the results obtained on SmCo/GdCo/SmCo' amorphous trilayers[5] are qualitatively close to the magnetic behavior described in this superlattice.

Finally, in the case where the YFe_2 layers are significantly thinner, for the same $DyFe_2$ thickness as in the superlattice *B* [superlattice *C*: $DyFe_2(100\,Å)/YFe_2$ (50 Å)], the hysteresis loops measured at low and room temperatures are given in

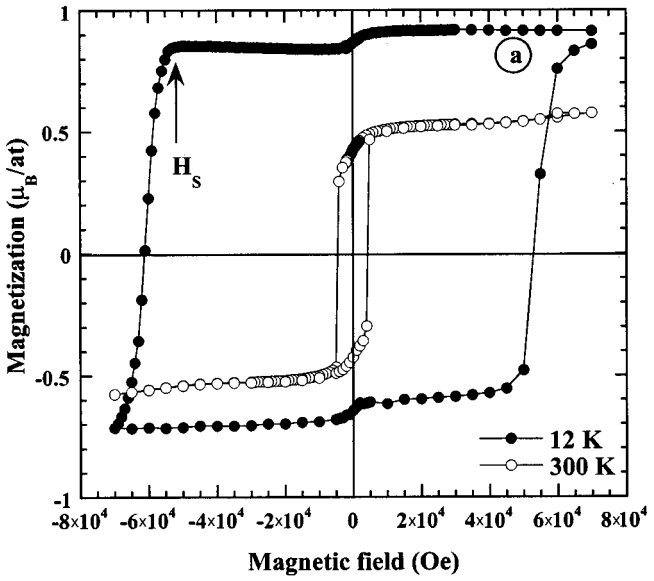

FIG. 6. Hysteresis loops measured at 12 K (black dots) and at room temperature (white dots) for the superlattice $[DyFe_2(100\,Å)/YFe_2(50\,Å)]_{26}$. The letter *a* presented in a circle refers to the magnetic configuration sketched in Fig. 1(a). H_s is the magnetic field at which the $DyFe_2$ magnetization starts to switch.

Fig. 6. The loops are square at any temperature, as for a single hard phase, with a coercive field of about 60 kOe at 12 K and 5 kOe at 300 K. The value at 12 K is close to the H_s field measured in superlattice *B*, but the value at room temperature is three times smaller. There is no signature of magnetic walls in the YFe_2 layers, and the magnetization reversal is completely governed by the anisotropy in the $DyFe_2$ layers. This is due to the fact that the magnetic walls have no room to develop in these thin YFe_2 layers, and, therefore, the YFe_2 magnetization is firmly stuck to the $DyFe_2$ one, through the negative interface exchange coupling between dysprosium and iron magnetic moments. Under high magnetic field, the magnetic configuration is stable with respect to the interface exchange interaction between YFe_2 and $DyFe_2$ iron moments, as in superlattice *A* field-cooled under 10 kOe. However, as the Dy magnetic moments are dominant, this leads to a higher remanence state, stabilized by the $DyFe_2$ anisotropy. The YFe_2 moments, initially pointing along negative field, are not affected by the magnetic field reversal. The giant ferrimagnetic superlattice behaves as a unique block with a one-step magnetization reversal, where the hard and soft magnetic layers switch as a unit.

In conclusion, we have elaborated composite systems based on hard and soft magnetic phases, which also present high crystalline quality, coherence, and, therefore, well defined magnetization directions. These are epitaxied intermetallic superlattices constituted of $DyFe_2$ and YFe_2. Both compounds are very similar in crystal structure but exhibit great differences in their magnetic properties, especially in the magnetic anisotropy. The intermetallic compounds are antiferromagnetically coupled at the interfaces, which permits us to experience systems with extremely rich properties. We investigated the interface coupling effects in changing the relative thicknesses, and we shown how it is possible to tailor the magnetization reversal process in these superlattices. The results obtained for the superlattice $DyFe_2$ (50 Å)/YFe_2 (130 Å) are especially very promising since it presents at low temperature a completely reversible (*M*-*H*) loop over the $(-7.5\,T/+7.5\,T)$ field range, starting under 7 T from a magnetic configuration that can be chosen by the cooling-field value. The reversal field changes sign with the magnitude of the cooling field, which may give some insight into the positive exchange bias phenomenon.

The magnetic investigation of these Laves phases superlattices is still in progress via polarized neutron scattering experiments in order to get microscopic evidence for their magnetic configurations. Moreover, other intermetallic compounds will be included in these composite systems: $TbFe_2$ and Terfenol-D, for their huge magnetostrictive properties, and $SmFe_2$ because of the different exchange interactions expected.

These single crystalline intermetallic superlattices appear to be suitable model systems to help in understanding open issues in exchange-spring magnetism and exchange biasing, both effects that are central phenomena in permanent magnets and spin-valve devices.

[1] F. Kneller and R. Hawig, IEEE Trans. Magn. **27**, 3588 (1991).
[2] J. Ding, P. G. McCormick, and R. Street, J. Magn. Magn. Mater. **124**, 1 (1993).
[3] R. Skomski and J. M. D. Coey, Phys. Rev. B **48**, 15 812 (1993).
[4] I. A. Al-Omari and D. J. Sellmyer, Phys. Rev. B **52**, 3441 (1995).
[5] S. Wüchner, J. C. Toussaint, and J. Voiron, Phys. Rev. B **55**, 11 576 (1997).
[6] S. Mangin, G. Marchal, C. Bellouard, W. Wernsdorfer, and B. Barbara, Phys. Rev. B **58**, 2748 (1998).
[7] E. E. Fullerton, J. Samuel Jiang, C. H. Sowers, J. E. Pearson, and S. D. Bader, Appl. Phys. Lett. **72**, 380 (1998).
[8] A. E. Clark, in *Handbook on the Physics and Chemistry of Rare Earths*, edited by K. Gschneider, Jr. and L. Eyring (North-Holland, Amsterdam, 1979), Vol. 2, Chap. 15.
[9] V. Oderno, C. Dufour, Ph. Bauer, K. Dumesnil, Ph. Mangin, and G. Marchal, J. Cryst. Growth **165**, 175 (1996).
[10] V. Oderno, C. Dufour, K. Dumesnil, Ph. Bauer, Ph. Mangin, G. Marchal, L. Henet, and G. Patrat, Europhys. Lett. **9**, 713 (1996).
[11] J. Nogues, D. Lederman, T. J. Moran, and I. K. Schuller, Phys. Rev. Lett. **76**, 4624 (1996).
[12] K. Dumesnil, A. Mougin, C. Dufour, and Ph. Mangin, J. Magn. Magn. Mater. **198-199**, 516 (1999).